

# STUDIES OF QUASI-STATIC FRACTURE USING ITERATED CONFORMAL MAPS

H. G. E. HENTSCHEL<sup>1</sup> & ITAMAR PROCACCIA<sup>2</sup>

<sup>1</sup>Dept of Physics, Emory University, Atlanta Georgia 30322, USA

<sup>2</sup>Dept. of Chemical Physics, The Weizmann Institute of Science, Rehovot, 76100, Israel

## ABSTRACT

We will discuss how the structure and stress fields around quasistatically growing fractures can be generated and analysed using iterated conformal mapping techniques. Iterated conformal maps provide a powerful new analytic tool for the study of free boundary problems in two dimensions generated by harmonic or biharmonic fields resulting in branched patterns with nontrivial geometries. In all cases the object of interest is the function which conformally maps the exterior of the unit circle to the exterior of the growing fracture. The complexity of the evolving interface is described by the dynamics of the conformal map. The latter is obtained as an  $n$ -iterate of a fundamental conformal map. This method allows for an efficient and accurate solution of the Lamé equations without resorting to lattice models. Typical fracture patterns exhibit increased ramification due to the increase of the stress at the tips. We find the roughness exponent of the experimentally relevant backbone of the fracture pattern crosses over from about 0.5 for small scales to about 0.75 for large scales, in excellent agreement with experiments.

## 1 INTRODUCTION

The manner in which interfacial structure develops in fractures is due to the intricate interplay between surface energy, plasticity and wear at short lengthscales with long range elastic stresses (Landau and Lifshitz [1], Fineberg and Marder [2]). The stress fields themselves controlled by both boundary conditions at the sample edges and by zero stress boundary conditions at the free fracture surfaces give rise to a complex conformal problem in elasticity theory (Muskhelishvili [3]). How the resulting ramified interface develops needs new mathematical methods, and one of the most powerful of these are iterative conformal maps (Hastings and Levitov [4]). Iterated conformal maps (ICMs) have already been extensively studied in the context of laplacian flows and diffusion limited aggregation (Davidovitch *et al* [5]). In this paper we will describe initial work that suggests that ICMs will prove equally powerful in the context of fracture dynamics (Barra *et al* [6, 7]).

The reason for the power of ICMs lies in the fact that an algorithm is given for actually constructing the conformal map in an efficient computational manner. The usual difficulty when using conformal mapping techniques lies in the fact that while the solution to a physical problem (for example solving Laplaces equation  $\nabla^2\phi = 0$ ) can easily be expressed in terms of a conformal mapping  $z = \Phi(\omega)$  between a simple mathematical complex plane  $\omega$  and the physical plane  $z = x + iy$ , the mapping itself is almost impossible to find if the pattern is complex. For example, if we can solve for the complex potential  $V(\omega) = \phi + i\psi$ , describing our diffusive field in the mathematical plane, then we know that our diffusion equation has the solution  $\phi(x, y) = \Re[V(\Phi^{-1}(z))]$  in the physical plane. Ofcourse what we have really done is transfer all the complexity of the original problem into solving for the mapping  $z = \Phi(\omega)$ . We will describe here how such conformal maps can be built up iteratively using ICMs and use an example from Mode III quasi-static fracture to show their power.

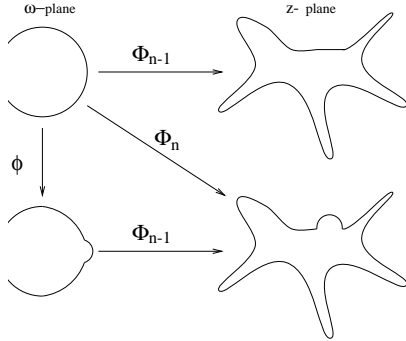


FIG. 1: Example of how to construct iteratively the conformal mapping from a circle to an arbitrarily shaped closed contour.

## 2 ITERATED CONFORMAL MAPS IN THE CONTEXT OF FRACTURE

We describe now how to construct in an iterative manner a conformal map from the complex  $\omega$ -plane to the physical  $z$ -plane such that the conformal map  $z = \Phi(\omega)$  maps the exterior of the unit circle in the  $\omega$ -plane to the exterior of the crack in the physical  $z$ -plane.

The essential building block in the present application, as in all the applications of the method of iterated conformal maps, is the fundamental map  $\phi_{\lambda,\theta}$  that maps the exterior circle onto the unit circle with a semi-circular bump of linear size  $\sqrt{\lambda}$  which is centered at the point  $e^{i\theta}$  [4]. By composing this map with itself  $n$  times with a judicious choice of series  $\{\theta_k\}_{k=1}^n$  and  $\{\lambda_k\}_{k=1}^n$  we can construct a mapping  $\Phi^{(n)}(\omega)$  from the exterior of the circle to the exterior of an arbitrary simply connected shape. To understand how to choose the two series  $\{\theta_k\}_{k=1}^n$  and  $\{\lambda_k\}_{k=1}^n$  consider Fig. 1. Assume now that we already have  $\Phi^{(n-1)}(\omega)$  we want to perform the next iteration. To construct  $\Phi^{(n)}(\omega)$  we first add a bump of an appropriate size and at an appropriate position, dependent on the physics involved, to the unit circle in the  $w$ -plane and then apply  $\Phi^{(n-1)}(\omega)$  to the new shape:

$$\Phi^{(n)}(\omega) = \Phi^{(n-1)}(\phi_{\theta_n,\lambda_n}(\omega)) . \quad (1)$$

The magnitude of the bump  $\lambda_n$  is determined by requiring fixed size bumps in the  $z$ -plane. This means using the Jacobian of the mapping that

$$\lambda_n = \frac{\lambda_0}{|\Phi^{(n-1)'}(e^{i\theta_n})|^2} . \quad (2)$$

Iterating this scheme we end up with a conformal map written in terms of an iteration over the fundamental maps:

$$\Phi^{(n)}(w) = \phi_{\theta_1,\lambda_1} \circ \dots \circ \phi_{\theta_n,\lambda_n}(w) . \quad (3)$$

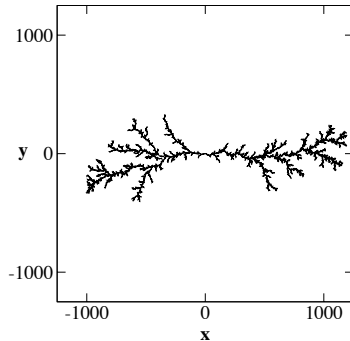


FIG. 2: A typical fracture pattern that is obtained from iterated conformal maps. What is seen is the boundary of the fractured zone, which is the mapping of the unit circle in the mathematical domain onto the physical domain. Notice that the pattern becomes more and more ramified as the fracture pattern develops. This is due to the enhancement of the stress field at the tips of the growing pattern

The appropriate angle  $\theta_k$  depends on the physics we wish to describe and will be discussed further below in the context of fracture.

### 3 HARMONIC MODE III FRACTURES

Although we can develop the approach described above in full generality [7], for the sake of clarity we will here consider mode III fracturing [6] for which a 3-dimensional elastic medium is subjected to a finite shear stress  $\sigma_{zy} \rightarrow \sigma_\infty$  as  $y \rightarrow \pm\infty$ . Such an applied stress will create a harmonic displacement field  $u_z(x, y)$ ,  $u_x = 0$ ,  $u_y = 0$  in the medium. Despite the medium being three dimensional, therefore, the calculation of the strain and stress tensors are two dimensional.

We can describe a crack of arbitrary shape by its interface  $\vec{x}(s)$ , where  $s$  is the arc length which is used to parameterize the contour. We wish to develop a quasi-static model for the time development of this fracture in which discrete events advance the interface with a normal velocity

$$v_n(s) = \alpha(|\sigma_{zt}(s)| - \sigma_c) \quad (4)$$

if the transverse component of the stress tensor  $\sigma_{zt}$  is greater than a critical yield value  $\sigma_c$  for fracturing; otherwise no fracture propagation occurs. We will use the notation  $(t, n)$  to describe respectively the transverse and normal directions at any point on the two-dimensional crack interface. Whenever the interface has more than one position  $s$  for which  $v_n(s)$  does not vanish, we will respect the disorder by choosing the next growth position randomly with a probability proportional to  $v_n(s)$ . There we extend the crack by a fixed area of the size of the “process zone”  $\lambda_0$ , and therefore the required  $\lambda_n$  are given by eqn 3.

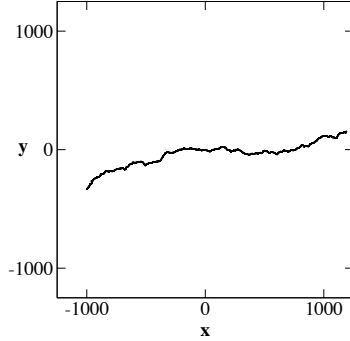


FIG. 3: A typical backbone of the fracture pattern. This is the projection onto the x-y plane of the experimentally observed boundary between the two parts of the material that separate when the fracture pattern hits the lateral boundaries

In mode III fracture  $\nabla \cdot \mathbf{u} = 0$ , and the Lamé equation reduces to Laplace's equation

$$\partial^2 u_z / \partial x^2 + \partial^2 u_z / \partial y^2 = 0, \quad (5)$$

and therefore  $u_z$  is the real part of an analytic function

$$\chi(z) = u_z(x, y) + i\xi_z(x, y) \quad (6)$$

where  $z = x + iy$ . The boundary conditions far from the crack and on the crack interface can then be used to find this analytic function on the unit circle

$$\chi^{(0)}(\omega) = -i[\sigma_\infty / \mu](\omega - 1/\omega) \quad (7)$$

Now invoke a conformal map  $z = \Phi^{(n)}(\omega)$  that maps the exterior of unit circle in the mathematical plane  $\omega$  to the exterior of the crack in the physical plane  $z$ , after  $n$  growth steps. This conformal map is univalent by construction, and therefore admits a Laurent expansion

$$\Phi^{(n)}(\omega) = F_1^{(n)}\omega + F_0^{(n)} + F_{-1}^{(n)}/\omega + F_{-2}^{(n)}/\omega^2 + \dots \quad (8)$$

Then the required analytic function  $\chi^{(n)}(z)$  is given by the expression

$$\chi^{(n)}(z) = -i[F_1^{(n)}\sigma_\infty / \mu] \left( \Phi^{(n)-1}(z) - 1/\Phi^{(n)-1}(z) \right) \quad (9)$$

From this we can now compute the transverse stress tensor:

$$\sigma_{zt}(s) = \mu \partial_t u_z = 2\sigma_\infty F_1^{(n)} \frac{\cos \theta}{|\Phi'^{(n)}(e^{i\theta})|}, \quad (10)$$

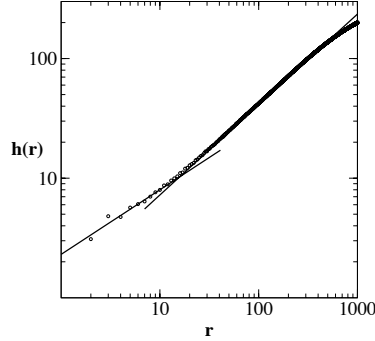


FIG. 4:  $h(r)$  averaged over all the backbone and over 70 fracture patterns each of which of 10 000 fracture events. There is a cross-over between a scaling law with roughness exponent  $0.54 \pm 0.05$  to and exponent of  $0.75 \pm 0.02$

on the boundary, and therefore we will have an explicit expression for the fracture growth from eqn 4 once the correct distribution of  $\Phi^{(n)}(\omega)$  is obtained.

Suppose that  $\Phi^{(n-1)}(\omega)$  is known, with  $\Phi^{(0)}(\omega)$  being the identity,  $\Phi^{(0)}(\omega) = \omega$ . We first compute the transverse strain tensor  $\sigma_{zt}(\theta) = 2\sigma_{\infty}F_1^{(n-1)}\cos\theta/|\Phi'^{(n-1)}(e^{-i\theta})|$ . In order to grow according to the requirement (4), we should choose growth sites more often when  $\Delta\sigma(\theta) \equiv \sigma_{zt}(\theta) - \sigma_c$  is larger. We therefore construct a probability density  $P(\theta)$  on the unit circle  $e^{i\theta}$  which satisfies

$$P(\theta) = \frac{|\Phi'^{(n-1)}(e^{i\theta})|\Delta\sigma(\theta)\Theta(\Delta\sigma(\theta))}{\int_0^{2\pi} |\Phi'^{(n-1)}(e^{i\tilde{\theta}})|\Delta\sigma(\tilde{\theta})\Theta(\Delta\sigma(\tilde{\theta}))d\tilde{\theta}}, \quad (11)$$

where  $\Theta(\Delta\sigma(\tilde{\theta}))$  is the Heaviside function, and  $|\Phi'^{(n-1)}(e^{i\theta})|$  is simply the Jacobian of the transformation from mathematical to physical plane. The next growth position,  $\theta_n$  in the mathematical plane, is chosen randomly with respect to the probability  $P(\theta)d\theta$ .

A typical fracture pattern that is obtained with this theory after 10 000 growth events is shown in Fig. 2. The fracture pattern begins with very low ramification when the stress field exceeds the threshold value only at few positions on the fracture interface. Later it evolves to a much more ramified pattern due to the increase of the stress fields at the tips of the mature pattern. *The scaling properties of the backbone reflect this cross-over* In Fig. 3 we show the backbone of the pattern displayed in Fig. 2.

We measure, for any given  $r$ , the quantity [8]

$$h(r) \equiv \langle \text{Max}\{y(r')\}_{x < r' < x+r} - \text{Min}\{y(r')\}_{x < r' < x+r} \rangle_x. \quad (12)$$

The roughness exponent  $\zeta$  is then obtained from

$$h(r) \sim r^\zeta, \quad (13)$$

if this relation holds. To get good statistics we average, in addition to all  $x$  for the same backbone, over many fracture patterns. The result of the analysis is shown in Fig. 4. We find that the roughness exponent for the backbone exhibits a clear cross-over from 0.54 for shorter distances  $r$  to 0.75 for larger distances. Within the error bars these results are in excellent agreement with the numbers quoted experimentally, see for example [8].

### Acknowledgments

This work has been supported in part by the Petroleum Research Fund, The European Commission under the TMR program and the Naftali and Anna Backenroth-Bronicki Fund for Research in Chaos and Complexity.

- 
- [1] Landau L.D. and Lifshitz E.M., *Theory of Elasticity*, 3rd ed. (Pergamon, London, 1986).
  - [2] Fineberg J. and Marder M., Instability in Dynamic Fracture, *Phys. Rep.* **313**, 1, (1999), and references therein.
  - [3] Muskhelishvili N.I. , *Some Basic Problems in the Mathematical Theory of Elasticity*, (Noordhoff, Groningen, 1952).
  - [4] Hastings M.B. and Levitov L.S., Laplacian Growth as One Dimensional Turbulence, *Physica D* **116**, 244 (1998).
  - [5] Davidovitch B., Hentschel H.G.E., Olami Z., Procaccia I., Sander L.M. , and Somfai E. , Diffusion limited aggregation and iterated conformal maps, *Phys. Rev. E*, **59** 1368 (1999).
  - [6] Barra F., Hentschel H.G.E., Levermann A., Procaccia I., Quasi-Static Fractures in Brittle Media and Iterated Conformal Maps. *Phys. Rev. E* **65**, 045101 (2002).
  - [7] Barra F., Levermann A. and Procaccia I., Quasistatic Brittle Fracture in Inhomogeneous Media and Iterated Conformal Maps: Modes I, II, III *Phys. Rev. E* **66**, 066122 (2002).
  - [8] Bouchaud E., J. Scaling properties of cracks, *Phys: Condens. Matter* **9**, 4319 (1997).